



Original Research Article

Application of a New Polymer Agcl Nanoparticles Coated Polyethylene Terephthalat [PET] as Adsorbent for Removal and Electrochemical Determination of Methylene Blue Dye

Mitra Alidadykhah, Hossein Peyman*, Hamideh Roshanfekar

Department of chemistry, Ilam branch, Islamic Azad University, Ilam, Iran

ARTICLE INFO

Article history

Submitted: 2020-10-16

Revised: 2020-11-04

Accepted: 2020-11-24

Manuscript ID: CHEMM-2010-1292

DOI: [10.22034/chemm.2021.119677](https://doi.org/10.22034/chemm.2021.119677)

KEYWORDS

Polyethylene terephthalate

Methylene blue removal

AgCl nanoparticles

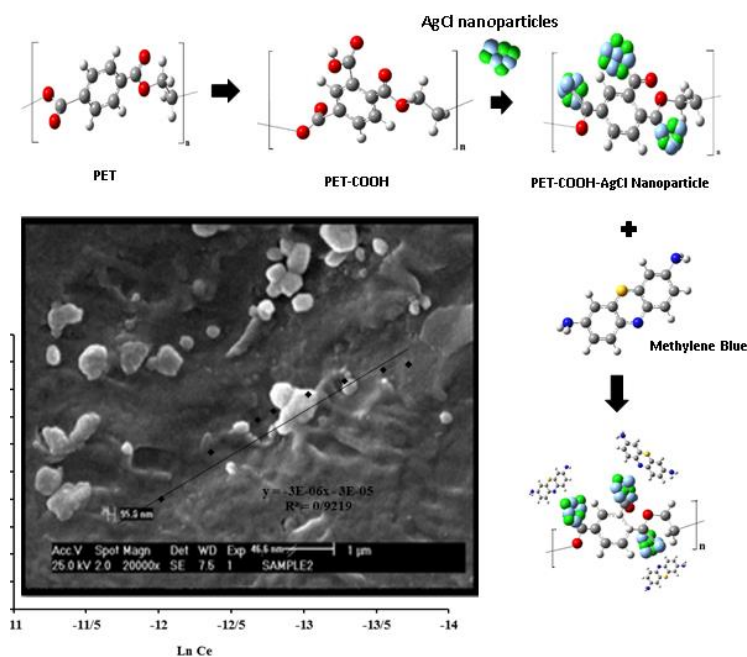
Adsorbent

Nanocomposite

ABSTRACT

In this study, two efficient applications for a novel modified polymer (polyethylene terephthalate [PET] modified with AgCl nanoparticles) were proposed and experimentally evaluated. First, PET-AgCl NPs were applied as an adsorbent to remove methylene blue (MB) dye, and the effect of pH, incubation time, concentration of MB, and temperature on the dye removal were studied and optimized to improve dye removal efficiency. The optimum condition included pH 9, temperature 45 °C, and incubation time 24 h. The adsorption fitted the Temkin isotherm model. In the other part of the study, a composite of PET-AgCl NPs with multiwall carbon nanotubes (MWCNTs) was used to modify the gold electrode in order to detect MB dye. The modified electrode exhibited a linear detection range, 5 μM to 10 nM, with a detection limit of 4.6 nM.

GRAPHICAL ABSTRACT



* Corresponding author: Hossein Peyman

✉ E-mail: peymanhossein@gmail.com

© 2020 by SPC (Sami Publishing Company)

Introduction

In recent years, the world has encountered environmental pollutants that one of which is colored wastewater [1-3]. Approximately one million ton of dye is produced annually in cosmetics, leather, paper, and textile industries. This huge amount of dye production has led to produce a lot of effluent containing dye and from an environmental perspective, it needs to be measured and filtered effectively [4-7]. Since the effluent from textile industries contains organic compounds such as dyestuffs, they have been considered as a serious environmental problem. Due to the structural variety and complexity of these molecules, they are potential sources of environmental pollution worldwide [8].

One of the most common dyes in textile industry is methylene blue (MB) that is a cationic dye and has a high water solubility [9]. MB is a cationic thiazine dye that is light blue in normal form and dark blue in oxidation form [10]. It has multiple aromatic rings and due to the toxicity, it can cause respiratory problems (in case of inhaling), irritation, nausea (in case of swallowing), vomiting, diarrhea, and gastroenteritis symptoms. Swallowing too much MB dye leads to headache, chest pain, dizziness, and syndromes like methemoglobinemia [11]; therefore, MB dye removal is very important. Moreover, MB has been known as a criterion for dye removal in dye studies.

In order to eliminate such compounds, different methods such as coagulation/flocculation, biological filtering, chemical oxidation, electrochemical filtering, ion exchanging, and surface absorbing have been applied [8, 12, 13]. Surface adsorption can be considered as a very effective and applicable technique to remove textile effluents, because the colored compounds in wastewater can be easily transferred to solid phase and the adsorbent can be reused by reduction and kept safely [14].

Although, adsorption technique provides several benefits such as low cost, easy to design and use, and no sensitivity to toxic compounds, it has some limitations including high cost of the

adsorbents, so choosing the adsorbent can be an important factor, especially in industrial application.

Polyethylene terephthalate (PET) is a linear and aromatic polyester that is the product of reaction between terephthalic acid and ethylene glycol [8, 9, 15]. This polymer is widely used in medical applications such as vascular prostheses [16-19], heart valve sewing cuffs [12, 13, 20], implantable sutures [21, 22] and other surgical usage [23, 24].

As an inert polymer with no reactive surface functional groups, modification of PET surface can improve its biocompatibility. So, we functionalized the PET surface with carboxyl groups for immobilization of AgCl nanoparticles that could improve the desirable properties of PET. This immobilization was done by sonochemistry method [25]. Thus, PET surface was functionalized with carboxyl groups and then, AgCl nanoparticles were immobilized using sonochemistry method to improve the desirable properties of PET.

Now, in the current work we used this novel synthesized polymer PET-AgCl NPs as adsorbent and electrode modifier. Electrochemical measurement is one of the best methods for detection and determination of different material because of high sensitivity and selectivity, high response speed and low cost [26-28]. In first section, it was investigated if this new polymer could be a proper adsorbent for MB removal or not and after that the effect of different variables on dye removal was studied. In second section, we studied the role of this polymer as electrode modifier for electrochemical determination of MB dye. In order to perform electrochemical analyses, different electrodes such as gold and glassy carbon electrode can be used. In this study, according to the potential area used and better and more stable connection of the polymer to the surface of the gold electrode, this electrode modified by carbon nano tube (CNT) and nano composite was used [29-31].

Material and methods

All the materials were purchased from Merck Co., Germany, without further purification (HPLC grade). A double-beam UV-Vis spectrophotometer (model lambda 25, Perkin Elmer) was used to obtain MB spectra and evaluate its removal by polyethylene terephthalate (PET) modified with AgCl nanoparticles. All the voltametric experiments were done using potentiostat/galvanostat μ Auto lab Type III (FRA 2) with a single cell containing three electrodes: The gold electrode as a working electrode, the calomel electrode as a reference electrode, and the platinum as a counter electrode. All the electrodes were obtained from Metrohm Co.

Synthesis of PET modified with AgCl nanoparticles

The modification process was done in two steps: First, PET was functionalized with carboxyl groups by immersing PET fibers in a solution of formaldehyde and acetic acid for 4 h in room temperature.

In the next step, PET was immersed in a solution of bromoacetic acid and NaOH for 18 h. Then, it was rinsed with distilled water and dried in oven [32] followed by being coated with nanoparticles. The growth of AgCl nanoparticles on the surfaces of carboxylated PET fibers was obtained by sequential dipping steps in alternating bath of potassium chloride and silver nitrate under ultrasound irradiation [18]. Scanning electronic microscopy (SEM) technique was applied to confirm the synthesis of modified PET (Figure 1).

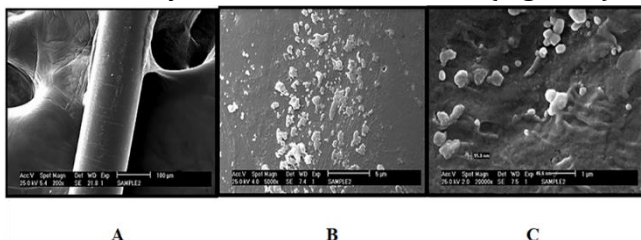


Figure 1: SEM images of A) blank PET B and C) modified PET with AgCl nanoparticles

Adsorption experiments

Synthesized PET-AgCl NPs polymer was used as an adsorbent to remove the cationic dye MB. In

all investigations, the UV-Vis spectra of MB solutions before and after addition of the PET-AgCl NPs as adsorbent was recorded. In each experiment, the percentage of dye removal was calculated according to Equation 1:

$$\% \text{ Removal} = \frac{A_b - A_f}{A_b} \times 100 \quad (1)$$

Where A_b and A_f are absorbance of MB in before and after incubation with modified PET, respectively.

The influence of experimental parameters such as incubation time, pH, temperature, adsorbent dosage and the MB concentration on removal efficiency were investigated. In each experiment, 100 ml solution containing 1×10^{-5} M MB and 0.02 g of modified PET were agitated on stirrer. The experimental data were analyzed to confirm the best-fit isotherms. The effect of incubation time was investigated in different time intervals using stirring MB solution (1×10^{-5} M) and modified PET (0.02 g) in room temperature and dark condition.

In order to evaluate the pH effect on MB removal, the same concentration of MB with different pH (5, 7, 8, 9, 11, and 12) was prepared. The solution pH was adjusted by addition of dilute solution of HCl and NaOH.

The absorption of each MB solution with known pH was recorded using UV-Vis spectrophotometer, then 0.02 g of modified PET (as an adsorbent) was added to each solution. After 24 h the UV-Vis spectra were obtained and compared with the spectra before MB dye removal.

To investigate the effect of initial concentration of MB on the dye removal, different concentrations of MB (0.5×10^{-5} , 0.8×10^{-5} , 1×10^{-5} , and 2×10^{-5} M) were used in optimum pH and the UV-Vis spectra of each sample were recorded without adsorbent. Then, the modified PET was added to MB solution and after 24 hours, the UV-Vis spectra of each sample were measured and compared with the UV-Vis of the samples before adding modified PET.

To study the effect of temperature on the MB dye removal by the PET modified with AgCl nanoparticles, 0.02 g of the modified PET was added to 5 ml MB solution, 1×10^{-5} M, in different temperatures (25, 35, 45, and 55 °C) for 24 h then, the UV-Vis absorption spectra of the samples were recorded and compared with the UV-Vis absorption of the samples before adding the adsorbent to obtain the percentage of the dye removal in different temperatures.

One of the other factors influencing the proper removal of a pollutant by an adsorbent is the weight of adsorbent. Therefore, constant concentrations of MB dye were contacted with different weights of PET-AgCl NPs (10-70 mg) and the amount of removal was obtained for each sample.

Electrochemical measurement of MB dye

Preparation of MWCNT/PET-AgCl nanocomposite

To synthesize the nanocomposite, the optimized amount of MWCNT, 1 mg modified PET, 0.1 g phenol as a polymer solvent, and 10 μ l water were mixed and the mixture was put in a water bath to solubilize the polymer and disperse carbon nanotube in melted phenol. Then, the composite was sonicated for 4 h to obtain homogenized composite.

Different amounts of MWCNT were used to obtain the optimized amount of MWCNT in composite. So, 0.4, 0.6, 1, 1.4, and 1.8 mg MWCNT were added to 1 mg modified PET, 0.1 g phenol, and 10 μ l water. The optimum conditions were applied during composite preparation. A proper composition is stable, homogenized, and uniformed and all materials in composite should form a homogenized phase. Therefore, the amount of carbon nanotubes should be chosen properly so as to form a stable composition with PET and phenol.

Fabrication of MWCNT/PET-AgCl/AuE

Before all the experiments, AuE was polished with 0.5 and 0.05 μ m alumina powder and rinsed with ethanol and double distilled water. Next, 10 μ l of MWCNT/PET-AgCl NPs nanocomposite was

put on the surface of the electrode and dried in room temperature (MWCNT/PET-AgCl NPs/AuE). For comparison 10 μ l of PET-AgCl NPs were used to fabricate PET-AgCl NPs/AuE.

Result and Dissection

Adsorbent characterization

As mentioned before, our adsorbent is a new modified polymer (PET-AgCl NPs) that we initially functionalized PET with carboxylate groups in two steps: First, in the presence of acetic acid and formaldehyde solution, $-\text{CH}_2\text{OH}$ group bonded to the aromatic ring and second, in the presence of sodium hydroxide and bromoacetic acid solution, $-\text{CH}_2\text{OH}$ group became deprotonated and changed into carboxylic acid group. Functionalized PET was characterized with FT-IR method (Figure 2) [33]. As shown in Figure 2, spectrum A is related to non-functionalized PET polymer and spectrum B is related to functionalized PET.

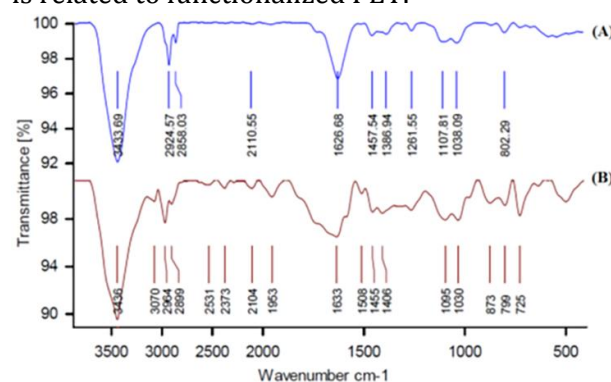


Figure 2: FT-IR spectrum of PET, A) Non-functionalized PET, B) Functionalized PET by acetic acid groups

In spectrum A, stretching vibrations of O-H at the end of PET polymer (3433.69 cm^{-1}), esteric C=O groups (1626.68 cm^{-1}), C-O group (1038.09 and 1107.81 cm^{-1}), C=C group of aromatic ring (1457.54 cm^{-1}), $\text{CH}_2\text{-CH}_2$ group (2858.03 and 2924.57 cm^{-1}), out of plane C-H (802.29 cm^{-1}) are shown.

The presence of esteric C=O groups in lower frequency (related to $1735\text{-}1750 \text{ cm}^{-1}$) is a result of being near the aromatic ring and its electron withdrawing nature. Besides, the due to the overlapping with spectra peak of esteric C=O

group (1600 cm^{-1}), the C=C group appears in 1457.54 cm^{-1} .

In the spectrum B, the peaks of functional groups of PET polymer ($-\text{COOH}$ functional group) appeared and stretching vibration of O-H at the end of polymer (3436 cm^{-1}), acidic O-H (3070 cm^{-1}), polymeric C=O (1633 cm^{-1}), and acidic C=O (1731 cm^{-1}) are shown. The frequency of esteic C=O group shifted to the frequency lower than acidic C=O due to the withdrawing substituent in the aromatic ring.

After successful functionalization of PET polymer, immobilization of AgCl nanoparticles on them was well done and was shown in Figure 1.

Adsorption process Study

Optimization of parameters

For adsorption studies, the proper amount of PET-AgCl NPs and MB dye were contacted against each other and in the certain time intervals, UV-Vis spectra were recorded and the dye removal percentage was calculated by Equation 1. The results showed that the modified polymer was able to adsorb MB dye and as shown in Figure 3, over time, the concentration of MB dye was decreased in solution because the dye adsorption on modified polymer was increased. Therefore, the absorption spectra showed a considerable decrease (Figure 3). After 24 hours, due to saturation of adsorbent surface with dye, the concentration of MB in solution became constant; therefore, UV-Vis spectra were leveled off.

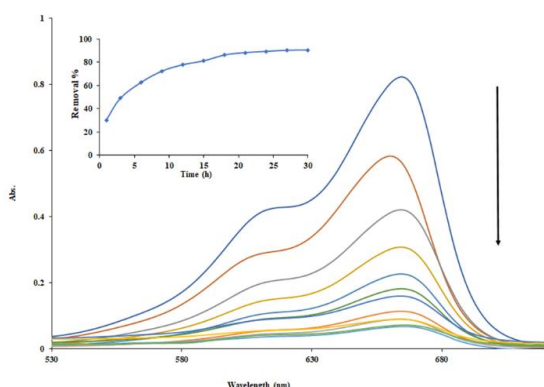


Figure 3: UV-Vis spectrums of MB ($10\text{ }\mu\text{M}$) in present of PET-AgCl NPs (0.02 g) in different times. Inset) Removal percentage of MB by PET-AgCl NPs by time increasing

In the pH effect study, percentage of dye removal was calculated in different pHs (Figure 4). The results were 9.76%, 24.69%, 31.92%, 94.22 %, 53.33 %, and 26.82% for pH 5, 7, 8, 9, 11, and 12 respectively. According to the maximum dye removal, pH 9 was selected as the optimum pH. The increase in dye removal by increasing pH can be explained according to MB structure (scheme 1), in acidic condition, the surface of both adsorbent and dye are protonated causing repulsion force to decrease in dye removal. On the other hand, in alkaline condition, the surface of the dye and the adsorbent is deprotonated; therefore, the possibility of dye attachment to the adsorbent surface increased. But at high pH conditions, the competition between the dye and the OH^- group for adsorption on PET-AgCl NPs reduced the rate of dye removal.

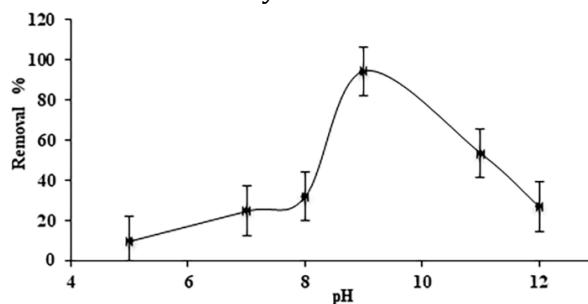
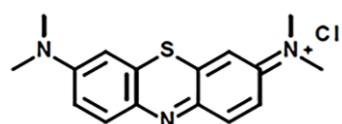


Figure 4: MB ($10\text{ }\mu\text{M}$) removal percent curve by PET-AgCl NPs (0.02 g) in different pH (5, 7, 8, 9, 11, and 12)



Scheme 1: MB structure

In the other part of our study, the effect of different concentrations of MB on removal process was evaluated (Figure 5). The removal percentages of dye were obtained by 95.81%, 53.14%, 50.68%, and 21.55% for 5, 8, 10, and 20 μM of MB dye, respectively.

The percentage of MB dye removal decreased with the increase in the MB dye concentration, because the increase in initial concentration led to decrease in the attachment possibility and resulted in decreased removal percentage of the dye.

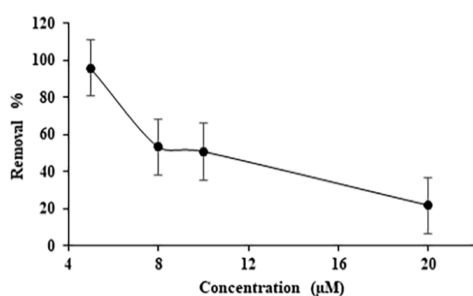


Figure 5: MB removal percent curve by PET-AgCl NPs (0.02 g) in different concentration of MB (5, 8, 10, and 20 µM)

The decreased removal of the dye in the higher concentrations may be due to the monolayer mechanism of interaction. In a high concentration of dye, the first layers became quickly occupied; therefore, there was no more capacity to adsorb more dye and dye removal decreased. On the other hand, in the samples with lower dye concentration, the possibility of attachment increased that led to enhance the dye adsorption.

The percentages of dye removal in different temperatures were obtained by 52.61%, 71.84%, 98.62%, and 81.61% for 25, 35, 45, and 55 °C respectively (Figure 6). According to the results, the mechanism of adsorption was exothermic and the optimum temperature to remove the MB dye by the modified PET was 45 °C. Increased temperature up to 45 °C provided the activation energy for adsorption leading to increased removal percent and more dye molecules could be adsorbed, but exothermic nature of adsorption process resulted in weakened attachment of dye to polymer surface; therefore, the adsorption decreased.

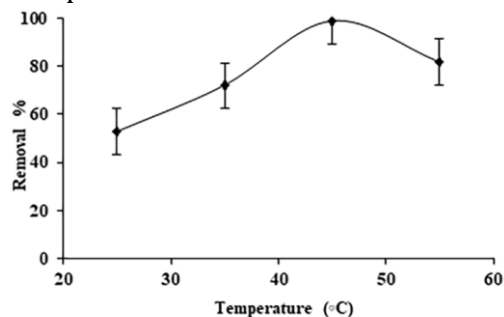


Figure 6: MB (10 µM) removal percent curve by PET-AgCl NPs (0.02 g) in different temperatures (25, 35, 45, and 55 °C)

Figure 7 indicates the results of the effect of adsorbent weight on adsorbent process. According to the results, it can be concluded that by increasing the amount of adsorbent, the percentage of removal increased that can be related to the sharp increase in the surface area of the adsorbent. But after the maximum removal, due to the constant amount of removable material, there was no significant increase in the effective removal percentage by increasing the adsorbent area and the maximum removal reached in 0.03 g of adsorbent at 50 µM MB.

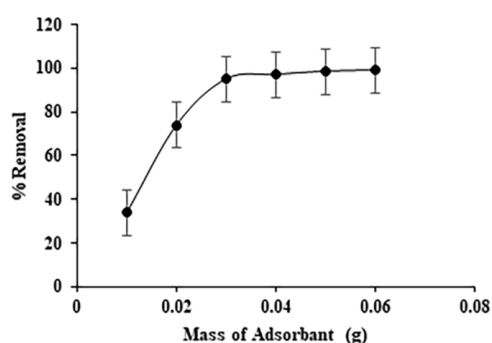


Figure 7: Removal percentage of MB by PET-AgCl NPs at 50 µM MB and pH 9 and different amount of adsorbent (0.01, 0.02, 0.03, 0.04, 0.05 and 0.06 g)

A possible explanation is that the adsorption is carried out on the adsorbent surface, increasing the amount of adsorbent and the available adsorbent surface; therefore, the removal percentage rises. After reaching the maximum removal of pollutants, increasing in adsorbent amount will not have any effect on increasing the removal percentage. Regarding the cost of the materials and synthesis of adsorbents, knowing the adsorbent weight ratio to the pollutant can help calculate the minimum amount of adsorbent needed for maximum removal of dye.

The equilibrium adsorption isotherms

The characteristics of adsorption can be defined by the equilibrium adsorption isotherms. The criterion for choosing the optimum isotherm is correlation coefficient (R^2). In the current study, the behavior of modified PET adsorbent was evaluated according to Langmuir, Freundlich, and Temkin isotherms [34].

Equation 2 shows Langmuir isotherm:

$$\frac{c_e}{q_e} = \frac{1}{bq_m} + \frac{c_e}{q_m} \quad (2)$$

Where C_e is the dye concentration and q_e is the equilibrium adsorption capacity according to equation 3:

$$q_e = (C_0 - C_e) \frac{V}{W} \quad (3)$$

Where C_0 and C_e are the initial and equilibrium dye concentrations in solution, respectively, V is the volume of the solution, and W is the mass of the adsorbent. The amount of b and q_m can be obtained from the slope $1/q_m$, and the y-intercept of plot C_e versus q_e ($q_m = 0.000002$ and $b = 66666.7$) (Figure 8).

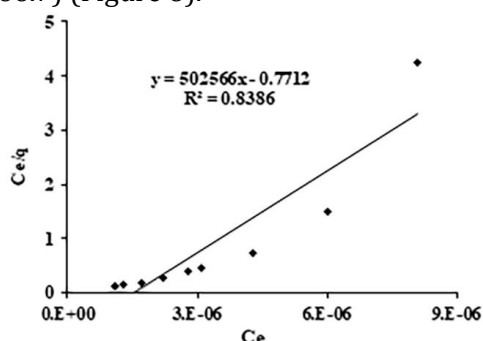


Figure 8: Conformance chart with Langmuir isotherm model

Equation 4 indicates Freundlich isotherm:

$$\ln q_e = \ln k_f + \frac{1}{n_f} \ln c_e \quad (4)$$

Where C_e represents the dye concentration and q_e indicates the equilibrium adsorption capacity. K_f and n_f are the Freundlich constants related with absorption intensity and adsorption capacity, respectively that can be obtained using the slope $1/n_f$, and y-intercept, $\ln k_f$, of plot $\ln q_e$ versus $\ln C_e$ ($n_f = 1.62$, $k_f = 2.25 \times 10^{-9}$) (Figure 9).

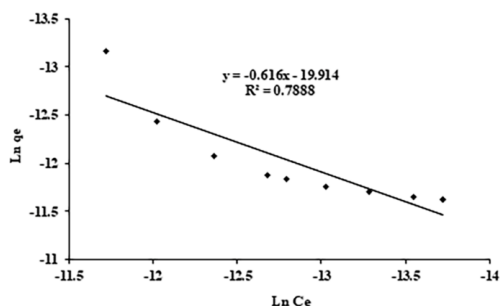


Figure 9: Conformance chart with Freundlich isotherm model

The following equation 5 shows Temkin isotherm:

$$q_e = B_1 \ln K_T + B_1 \ln C_e \quad (5)$$

Where C_e represents the dye concentration and q_e indicates the equilibrium adsorption capacity. K_T is equilibrium bonding constant related to maximum bonding energy, and B_1 is a constant related to absorption heat. K_T and B_1 can be obtained using the slope and y-intercept of plot q_e versus $\ln C_e$ ($B_1 = -3 \times 10^{-5}$, $K_T = 22026/5$) (Figure 10).

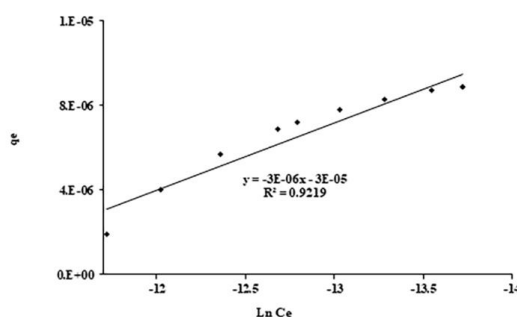


Figure 10: Conformance chart with Temkin isotherm model

Table 1, represents the studied models of isotherms. The experimental process was not fitted to Langmuir and Freundlich models; however, it was fitted to Temkin model very well with maximum R^2 .

Table 1: The results obtained from the study of matching three isotherm models with research

Models of isotherms	R^2	
Langmuir	0.8386	$b = -666666.7$ $q_m = 0.000002$
Freundlich	0.7888	$k_f = 2.25 \times 10^{-9}$ $n_f = 1.62$
Temkin	0.9219	$K_T = 22026.5$ $B_1 = -05 \times 10^{-3}$

Electrochemical Determination of MB by PET-AgCl NPs modified electrode

Composite optimization

As shown in Figure 11, the composite containing 1 mg carbon nanotubes is the most stable and considered as the optimized composite. The amount of carbon nanotubes lower than 1 mg is not acceptable due to making non-homogenous

and non-uniform composite. As a result of high amount of carbon nanotube, those composites consisting more than 1 mg carbon nanotube are not stable and form two separated phases after a short time.

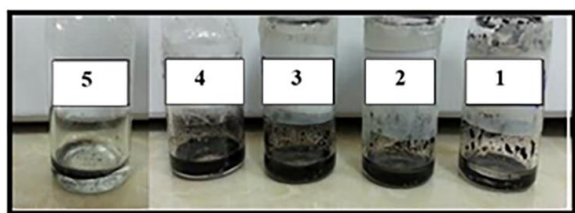


Figure 11: Composite 1 mg PET modified with AgCl nanoparticles and 0.1 g phenol with different values of non-functional CNTs, 1: 1.8, 2: 1.4, 3: 1, 4: 0.6 and 5: 0.4 mg

In this study, both functional and non-functional carbon nanotubes were used to make composite, but as shown in Figure 12, the composite consisting carboxyl group as functional carbon nanotubes is unstable and forms two separated phases. The instability may be due to the fact that the functional carbon nanotubes and PET make repulsion force that prevent their combination. Therefore, the non-functional carbon nanotubes were used to obtain a stable and homogenous composite.

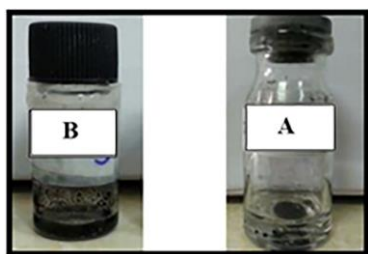


Figure 12: PET composite containing AgCl nanoparticles and CNTs A) functional CNTs and B) non-functional CNTs

Characterization of PET-AgCl NPs/ MWCNT modified electrode

In order to characterize electrode modification, the electrochemical behavior of bare AuE., PET-AgCl NPs/AuE and PET-AgCl NPs/ MWCNT/AuE was studied in phosphate buffer containing 5 mM $K_3[Fe(CN)_6]/K_4[Fe(CN)_6]$ (1:1 as redox probe) at 0.1 M KCl at room temperature. As shown in Figure 13, the bare electrode has a clear reversible redox curve. By casting PET-AgCl NP

on the surface of the electrode, due to polymer resistance, the redox peak current decreased. A slight electrical conductivity can be observed that is created by silver nanoparticles. Also, there is a significant shift to higher potentials that is due to the low-level electron transfer and resistance of PET-AgCl NPs composite. Adding MWCNT to PET-AgCl NP in PET-AgCl NPs/ MWCNT/AuE, caused a considerable increase in peak current that is attributed to the large surface area of MWCNT and its synergic effect with silver chloride nanoparticles.

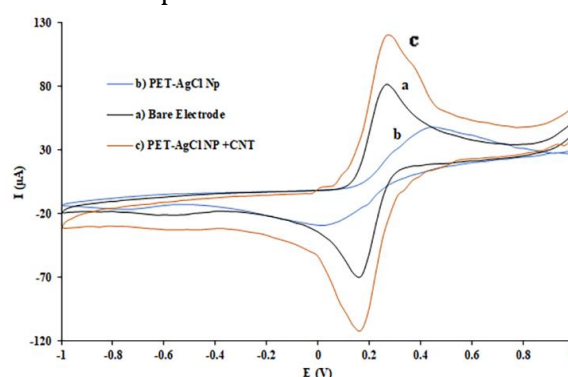


Figure 13: Cyclic voltammetry (CV) of a) Au Bare Electrode, b) PET-AgCl NPs/AuE, c) PET-AgCl NP+CNTs/AuE in 0.1M KCl and pH 9 PBS

pH optimization and electrochemical study of the composite

By considering the current difference in the presence and absence of analyte (MB dye) and obtaining the plot of current versus pH, it can be concluded that by increasing pH, the peak current will increase. At pH 9, there is a maximum current and at the pH above 9, the current decreases (Figure 14).

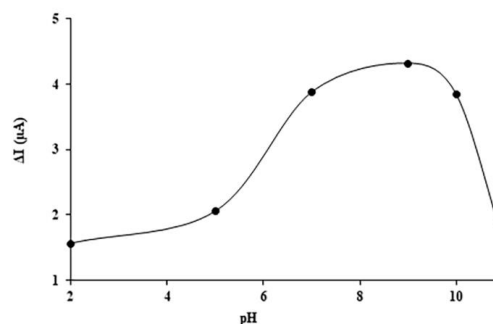


Figure 14: Peak current of MB (10 μ M) on PET-AgCl NP+CNTs/AuE in 0.1M KCl and different pH (2, 5, 7, 9, 10 and 11)

This phenomenon can be explained by stating that in acidic condition, because of existing protonated nitrogen and sulfur atoms in MB molecule there is less possibility for the attachment of MB to the surface of electrode, resulting in decreased current. On the other hand, at pH 9, MB molecule is deprotonated and the pair electron of nitrogen and sulfur atoms can bind to the metal of the electrode surface. At the pH higher than 9, there is a competition between the base molecules (OH^-) in the environment and MB molecule to bind to the surface of the electrode that results in decreased current. Therefore, pH 9 is the optimum pH due to the maximum current.

Study the effect of the potential scan rate

The redox peak current increases as the scan rate increases without considerable shift in the peak potentials. The plot of the peak current versus the potential scan rate (Figure 15A), and the plot of the peak current versus the square root of the potential scan rate (Figure 15B), with correlation coefficient (R^2) 0.8941 and 0.9857, respectively, show that the higher correlation coefficient in the plot of the peak current and the potential scan rate indicates that the electrochemical reaction is a diffusion control process at the surface of modified electrode [35].

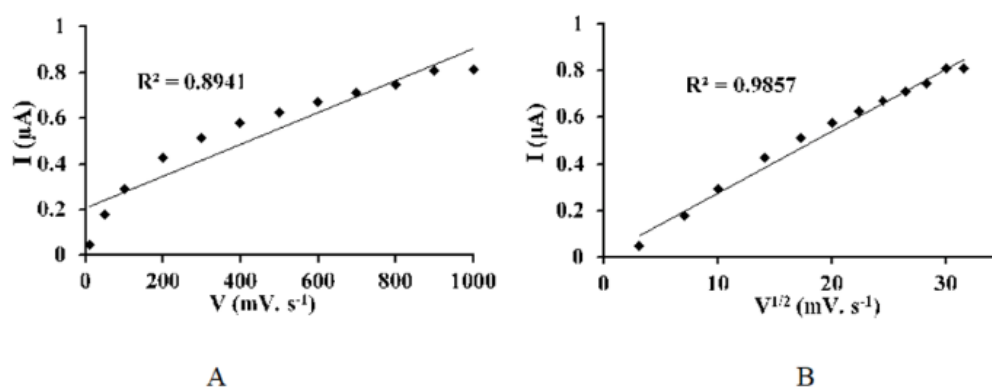


Figure 15: A) The plot of the peak current versus the potential scan rate, and B) the plot of the peak current versus the square root of the potential scan rate. Pick current of MB ($10 \mu\text{M}$) on PET-AgCl NP+CNTs/AuE in 0.1M KCl and pH 9

The quantitative range of electrochemical detection for MB is obtained. Figure 16 presents the effect of different concentrations of MB on the current response of PET-AgCl NPs-CNTs/AuE. It is clearly that the peak currents increased with the increasing of MB

concentration. The calibration curve displayed a linear range of $5 \mu\text{M}$ to 10 nM with a correlation coefficient of 0.998. The detection limit was 4.6 nM ($S/N = 3$) that compared with other works, proved acceptable obtained results (Table 2).

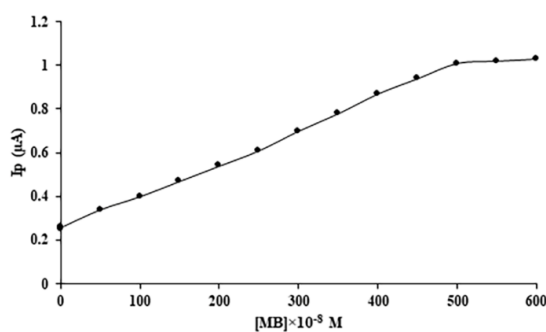


Figure 16: Calibration curve of MB on PEG-AgCl-CNT/AuE modified electrode in optimum condition

Table 2: Compression table

Method	Linear range	LOD	Reference
Salting-out assisted liquid-liquid extraction	0.2-7 mg/L	0.06 mg/L	[36]
Liquid chromatography-tandem mass spectrometry	1.0–20 µg/kg	0.5 µg/kg	[37]
Solid-phase extraction	0.36 and 1.08 µg/ml	0.1 ng/ml	[38]
Spectrophotometric	0.1–9.1 µg/ml	0.03 µg/ml	[39]
This study	1.6-3.2 µg/ml	1.5 µg/ml	

Conclusion

In this work, AgCl nanoparticles coated polyethylene terephthalate (PET) was synthesized via ultrasonic method and its application as MB dye absorbent was studied. The effective parameters on adsorption process were optimized: pH= 9, temperature = 45°C and $m_{\text{adsorbent}} = 0.03$ g. Also, the Langmuir, Freundlich, and Temkin isotherms were evaluated and regarding the correlation coefficient (R^2) values, the adsorption model fitted Temkin isotherm.

In other part of our study, electrochemical determination of MB with modified electrode by PET-AgCl NPs with multiwall carbon nanotube on gold electrode was investigated. The obtained linear range and detection limit are reasonable and our new modified polymer with the novel additives can be proposed for better electrochemical measurements.

Conflict of Interest

We have no conflicts of interest to disclose.

References

- [1]. Karimi-Maleh H., Kumar B.G., Rajendran S., Qin J., Vadivel S., Durgalakshmi D., Gracia F., Soto-Moscoso M., Orooji Y., Karimi F., *J. Mol. Liq.*, 2020, **314**:113588
- [2]. Karimi-Maleh H., Shafieizadeh M., Taher M.A., Opoku F., Kiarri E.M., Govender P.P., Ranjbari S., Rezapour M., Orooji Y., *J. Mol. Liq.*, 2020, **298**:112040
- [3]. Karimi-Maleh H., Fakude C.T., Mabuba N., Peleyeju G.M., Arotiba O.A., *J. Colloid Interface Sci.*, 2019, **554**:603
- [4]. Thomas O.E., Adegoke O., Kazeem A., Ezeuchenne I., *Prog. Chem. Biochem. Res.*, 2019, **2**:40
- [5]. Rezayati Zad Z., Moosavi B., Taheri A., *Adv. J. Chem. B*, 2020, **2**:159
- [6]. Khalil R., *Prog. Chem. Biochem. Res.*, 2020, **3**:269
- [7]. Rahimian R., Zarinabadi S., *Prog. Chem. Biochem. Res.*, 2020, **3**:251
- [8]. Dos Santos A.B., Cervantes F.J., van Lier J.B., *Bioresour. Technol.*, 2007, **98**:2369
- [9]. Royer B., Cardoso N.F., Lima E.C., Vagheti J.C., Simon N.M., Calvete T., Veses R.C., *J. Hazard. Mater.*, 2009, **164**:1213
- [10]. Miclescu A., Wiklund L., *J. Rom. Anest. Terap. Int.*, 2010, **17**:35
- [11]. Ponnusami V., Vikram S., Srivastava S.N., *J. Hazard. Mater.*, 2008, **152**:276
- [12]. Karagozoglu B., Tasdemir M., Demirbas E., Kobya M., *J. Hazard. Mater.*, 2007, **147**:297
- [13]. Nazari S., Yari A.R., Mahmodian M.H., Tanhaye R.M., Alizadeh M.S., Majidi G., Emamian M., *Arch. Hyg. Sci.*, 2013, **2**:104
- [14]. Lima E.C., Royer B., Vagheti J.C., Simon N.M., da Cunha B.M., Pavan F.A., Benvenutti E.V., Cataluña-Veses R., Airoidi C., *J. Hazard. Mater.*, 2008, **155**:536
- [15]. Royer B., Cardoso N.F., Lima E.C., Macedo T.R., Airoidi C., *J. Hazard. Mater.*, 2010, **181**:366
- [16]. Carneiro P.A., Umbuzeiro G.A., Oliveira D.P., Zandoni M.V.B., *J. Hazard. Mater.*, 2010, **174**:694
- [17]. de Lima R.O.A., Bazo A.P., Salvadori D.M.F., Rech C.M., de Palma Oliveira D., de Aragão Umbuzeiro G., *Mutat. Res. Genet. Toxicol. Environ. Mutagen.*, 2007, **626**:53
- [18]. Piccin J.S., Gomes C.S., Feris L.A., Gutterres M., *Chem. Eng. J.*, 2012, **183**:30
- [19]. Toor M., Jin B., *Chem. Eng. J.*, 2012, **187**:79
- [20]. Vandevivere P.C., Bianchi R., Verstraete W., *Environ. Clean Technol.*, 1998, **72**:289

- [21]. Anjaneyulu Y., Chary N.S., Raj D.S.S., *Rev. Environ. Sci. Technol.*, 2005, **4**:245
- [22]. Tünay O., Kabdasli I., Eremektar G., Orhon D., *Water Sci. Technol.*, 1996, **34**:9
- [23]. Allegre C., Moulin P., Maisseu M., Charbit F., *J. Membr. Sci.*, 2006, **269**:15
- [24]. Kapdan I.K., Kargi F., *Process Biochem.*, 2002, **37**:973
- [25]. Abbasi A.R., Morsali A., *Ultrason Sonochem.*, 2010, **17**:704
- [26]. Karimi-Maleh H., Karimi F., Orooji Y., Mansouri G., Razmjou A., Aygun A., Sen F., *Sci. Rep.*, 2020, **10**:1
- [27]. Karimi-Maleh H., Arotiba O.A., *J. Colloid Interface Sci.*, 2020, **560**:208
- [28]. Liu L., Yang H., *Int. J. Electrochem. Sci.*, 2020, **15**: 9658
- [29]. Heydarzadeh S., Roshanfekr H., Peyman H., Kashanian S., *Colloids Surf. A Physicochem. Eng. Asp.*, 2020, **587**:124219
- [30]. Rahimi F., Roshanfekr H., Peyman H., *Food Chem.*, 2020, **587**:124219
- [31]. Pyman H., Roshanfekr H., Ansari S., *Iran. Chem. Comm.*, 2020, **8**:52
- [32]. Filho H.J.I., dos Santos Salazar R.F., da Rosa Capri M., Neto Â.C., de Alcântara M.A.K., de Castro Peixoto A.L., State-of-the-Art and Trends in Atomic Absorption Spectrometry. *Atomic Absorption Spectroscopy*. InTech. 2012
- [33]. Muthuvijayan V., Gu, J., Lewis R.S., *Acta Biomater.*, 2009, **5**: 3382
- [34]. Dil E.A., Ghaedi M., Asfaram A., Mehrabi F., *Ultrason Sonochem.*, 2017, **36**: 409
- [35]. Aghajari R., Azadbakht A., *Anal. Biochem.*, 2018, **547**:57
- [36]. Razmara R.S., Daneshfar A., Sahrai R., *J. Ind. Eng. Chem.*, 2011, **17**:533
- [37]. Xu J.Z., Dai L., Wu B., Ding T., Zhu J.J., Lin H., Chen H.L., Shen C.Y., Jiang Y., *J. Sep. Sci.*, 2009, **32**:4193
- [38]. Khan M.R., Khan M.A., Alothman Z.A., Alsohaimi I.H., Naushad M., Al-Shaalan N.H., *RSC Adv.*, 2014, **4**:34037
- [39]. Corrigan O.I., Li X., *Sci. Pharm. J. Eur.*, 2009, **37**:477

HOW TO CITE THIS ARTICLE

Abdolkazem neisi, Neda Kayedi, Parviz Mahmoudi. Identification of Filamentous Microorganisms Causing Filamentous Bulking and Factors Affecting Their Growth in a Petrochemical Wastewater Treatment Plant, *Chem. Methodol.*, 2021, 5(2), 96-106

DOI: [10.22034/chemm.2021.119677](https://doi.org/10.22034/chemm.2021.119677)

URL: http://www.chemmethod.com/article_119677.html